Biochimica et Biophysica Acta 1817 (2012) 2060–2071

Contents lists available at SciVerse ScienceDirect

Biochimica et Biophysica Acta

journal homepage: www.elsevier.com/locate/bbabio

Oncosecretomics coupled to bioenergetics identifies α-amino adipic acid, isoleucine and GABA as potential biomarkers of cancer: Differential expression of c-Myc, Oct1 and KLF4 coordinates metabolic changes

Nadège Bellance [a,b], Lisa Pabst [a,b], Genevara Allen [c], Rodrigue Rossignol [d], Deepak Nagrath [a,b,e,*]

[a] Laboratory for Systems Biology of Human Diseases, USA
[b] Department of Chemical and Biomolecular Engineering, Rice University, Houston, TX, USA
[c] Department of Statistics, Rice University, Houston, TX, USA
[d] Univ. Bordeaux Maladies Rares, Génétique et Métabolisme (MRGM), EA 4576, F-33000 Bordeaux, France
[e] Department of Bioengineering, Rice University, Houston, TX, USA

ARTICLE INFO

Article history:
Received 19 March 2012
Received in revised form 23 June 2012
Accepted 19 July 2012
Available online 25 July 2012

Keywords:
Metabolism
Bioenergetics
Secretomics
Oxidative phosphorylation
Glycolysis

ABSTRACT

Bioenergetic profiling of tumors is a new challenge of cancer research and medicine as therapies are currently being developed. Meanwhile, methodological means must be proposed to gather information on tumor metabolism in order to adapt these potential therapies to the bioenergetic specificities of tumors. Studies performed on tumors and cancer cell lines have shown that cancer cells bioenergetics is highly variable. This profile changes with microenvironmental conditions (eg. substrate availability), the oncogenes activated (and the tumor suppressors inactivated) and the interaction with the stroma (i.e. reverse Warburg effect). Here, we assessed the power of metabolic footprinting (MFP) to unravel the bioenergetics and associated anabolic changes induced by three oncogenes, c-Myc, KLF4 and Oct1. The MFP approach provides a quantitative analysis of the metabolites secreted and consumed by cancer cells. We used ultra performance liquid chromatography for quantifying the amino acid uptake and secretion. To investigate the potential oncogene-mediated alterations in mitochondrial metabolism, we measured oxygen consumption rate and ATP production as well as the glucose uptake and lactate release. Our findings show that c-Myc deficiency initiates the Warburg effect along with a reduction of mitochondrial respiration. KLF4 deficiency also stimulated glycolysis, albeit without cellular respiration impairment. In contrast, Oct1 deficiency reduced glycolysis and enhanced oxidative phosphorylation efficiency. MFP revealed that c-Myc, KLF4 and Oct1 altered amino acid metabolism with specific patterns. We identified isoleucine, α-aminoadipic acid and GABA (γ-aminoisobutyric acid) as biomarkers related. Our findings establish the impact of Oct1, KLF4 and c-Myc on cancer bioenergetics and evidence a link between oncosecretomics and cellular bioenergetics profile.

1. Introduction

In the last decade, metabolic studies have revealed the existence of a large number of deregulations of the metabolic pathways involved in cancer cell's energy production, anabolism and tumor survival. For instance, cancer specific molecular changes were described at the level of hexokinase II (HK2), pyruvate dehydrogenase kinase 1 (PDK1), pyruvate dehydrogenase (PDH), isocitrate dehydrogenase (IDH1/2), ATP citrate lyase and lactate dehydrogenase isoforms (LDH) (see [1] and [2] for review). Three different metabolic remodeling have been reported in cancer cells based on the imbalance between the aerobic glycolysis and the oxidative phosphorylation. The phenotypes described were "highly glycolytic", "OXPHOS deficient" and "OXPHOS enhanced". These studies raised the question of the variability of cancer cell's bioenergetic profile and suggested to investigate further the variable modalities of energy production in tumors. This is a pre-requisite to select adapted tentative bioenergetics therapies targeted against the primary pathways of energy production and/or against the cancer-specific deviations of catabolism toward anabolism. The characterization of tumor bioenergetics profile necessitates tumor excision and both molecular and functional analyses in a microenvironment that mimics the tumor milieu. Moreover, as cancer cells express several oncogenes and since they grow in variable microenvironments, the complexity of cell's energetics is difficult to assess from the single measurements of ATP production by glycolysis and by oxidative phosphorylation in a chosen growth medium. Therefore, non-invasive technique should be developed in combination with bioenergetics profiling to better characterize tumor metabolism.

There is a need for alternative methodological means that could allow to derive relevant information on cancer energetics on a large number of samples. To this aim, we assessed here the potency of

* Corresponding author at: Department of Chemical and Biomolecular Engineering, Rice University, MS-362 Abercrombie Bldg, 6100 Main St, Houston, TX, 77251-1892, USA. Tel.: +1 713 348 6408; fax: +1 713 348 5478.
E-mail address: deepak.nagrath@rice.edu (D. Nagrath).

0005-2728/$ – see front matter © 2012 Elsevier B.V. All rights reserved.
http://dx.doi.org/10.1016/j.bbabio.2012.07.004

metabolic footprinting (MFP), a high throughput method for evaluating the metabolic changes that occur in the cellular secretome following the activation of specific oncogenes: c-Myc, KLF4 and Oct1 [3]. Whether specific changes in the tumor secretome, could provide a signature of particular oncogenes activation and of associated metabolic remodeling remains unknown. MFP is a powerful approach which helped recently to identify biomarkers predictive of diabetes [4]. We focused on the amino acids to gather information on the impact of c-Myc, Oct1 and KLF4 on the equilibrium between catabolism and anabolism. Recent studies revealed that carcinogenesis alters this equilibrium in favor of amino acid and lipid synthesis from glycolysis intermediates and TCA cycle metabolites, respectively [5]. Prior analysis of the metabolomics of prostate cancer or even colorectal cancer revealed important changes in amino acids [5,6]. However, the bioenergetic significance of these changes was not assessed. Furthermore, oncosecretomics could potentially help to identify the changes that occur at the level of energy metabolism in metabolic diseases other than cancer. Here we assessed in parallel the composition changes in the secreted metabolites and the deviations of energy production induced by oncogenes to assess the predictive potential of MFP.

2. Materials and methods

2.1. Cell types and culture conditions

The TGR-1 (c-Myc$^{+/+}$), HO15 (c-Myc$^{-/-}$) and HOMYC (HO15 + c-Myc) cells are rat fibroblasts and were obtained from Dr John Sedivy [7]. The wild-type mouse embryonic fibroblasts (MEFs) and Oct1$^{-/-}$ MEFs were obtained from Dr Dean Tantin [8]. The wild-type KLF4, KLF4$^{+/-}$ and KLF4$^{-/-}$ MEFs were provided by Dr Vincent Yang [9]. All cells were cultured in Dulbecco's modified eagle medium (DMEM) high glucose (GIBCO) containing 25 mM glucose, supplemented with 10% fetal calf serum (Invitrogen), 100 U/ml penicillin and streptomycin. All cells were kept in 5% CO_2 at 37 °C.

2.2. Cell proliferation

The cells were seeded at 10^4 cells per well in several 12 well plates. Cells were collected after every 24 h until 5 days. The collected cells were treated with 0.2% trypan blue in order to determine the viable cell number in each well.

2.3. Metabolic assays

The pyruvate uptake was estimated spectrophotometrically by measuring the remaining pyruvate in growth media after 24 h of incubation of the cells in different experimental conditions as specified in the text. The principle of the assay was to determine the amount of NADH oxidized at 340 nm on 96 well plates. Each well contained 20 μL of sample, NADH reagent, and lactate dehydrogenase reconstituted at 50% in glycerol and dilute at 1:20 in Tris (0.1 M, pH 7). After the incubation time, the cells were collected and lysed for protein determination (Pierce BCA Protein Assay kit). The results were then expressed in μmol/μg of protein as mean ± S.E.M. The lactate secretion was quantified with the lactate kit (Trinity biotech). The lactate secreted into the growth media by the cells after 24 h of incubation was measured according to the manufacturer's instructions. The absorbance at 540 nm was proportional to the lactate concentration in the sample. The results were expressed in μmol/μg of protein. By a similar method, the glucose consumption was determined with the Glucose Autokit (Wako).

2.4. ATP measurements

The intracellular ATP content was measured for the different cell types using the Cell Titer-Glo Luminescent cell viability assay (Promega). The cells were seeded in 96 well plates at 2.10^4 cells per well in 200 μL of high glucose DMEM medium. The following day, the media was replaced with 100 μL of high glucose DMEM without phenol red. The cells were then incubated for 1 h in either, the absence or the presence of oligomycin (2 μg/ml), 2-deoxyglucose (100 mM), or oligomycin plus 2-deoxyglucose, at 37 °C. The ATP content was thereby measured according to the manufacturer's instructions, with a spectrophotometer SpectraMax M5 (Molecular Devices).

2.5. Live/dead viability/cytotoxicity assay

The effect of 2DG on cell viability was quantified using the Live/Dead Viability/Cytotoxicity kit (*Invitrogen*). All the cells were seeded in 96 well plates at the same density as was done for the ATP measurements (2.10^4 cells per well). After an overnight incubation, cells were incubated in either 100 μL of DMEM high glucose, 100 mM 2DG or methanol (70%) for 1 h at 37 °C. At the end of the incubation time, cells were washed with PBS and treated with 0.5 μM Calcein AM and 1 μM Ethidium homodimer-1 for 30 min at 37 °C. Next, fluorescence was read at 517 nm for the live cells after an excitation of calcein AM at 494 nm. The amount of dead cells was determined by measuring the fluorescence emission at 617 nm produced via the excitation of ethidium homodimer-1 at 528 nm.

2.6. XF bioenergetic assay

Mitochondrial oxygen consumption was monitored with an XF24 *Extracellular flux Analyzer* (Seahorse Bioscience). The cells were seeded in Seahorse 24 well microplates at a cell density of 10^4 cells per well in 100 μL of assay media. The following day, after an overnight incubation at 37 °C with 5% CO_2, the cells were washed with PBS and then incubated in 200 μL of either high glucose DMEM for 24 h. For equilibration, the media was replaced with 850 μL of assay medium composed of high glucose DMEM medium (25 mM glucose, 4 mM glutamine and 1 mM pyruvate, without serum and sodium bicarbonate) and incubated at 37 °C without CO_2 for 1 h. The endogenous respiration or basal oxygen consumption rate (OCR) was then measured. The endogenous coupling degree of the OXPHOS system was assessed using oligomycin (2 μg/ml), an inhibitor of the F_1F_O-ATPsynthase. The uncoupled OCR was also measured in presence of 2.5 μM of FCCP. Finally, the cells were treated with a mitochondrial complex III inhibitor, antimycin A in order to assess the mitochondrial contribution to OCR.

2.7. Western blot

Cell lysis was performed using 4% laurylmaltoside as a detergent with each cell suspensions containing PBS and protease inhibitors (PMSF, Pepstatin A and Leupeptin). Antibodies against the respiratory chain complexes were obtained from *Mitosciences*. The anti β-actin, anti-GLUT1 and anti-ASCT2 antibodies were purchased from *SantaCruz Biotechnology*. The signal was detected using the chemiluminescent ECL PlusTM reagent (*Amersham*), and subsequently quantified with densitometric analysis using Image J software (NIH).

2.8. UPLC

Media samples were collected after 24 h of incubation and were stored at −80 °C. Extracellular metabolite profiling was performed using a Waters ACQUITY UPLC system. Each media sample was prepared according to the manufacturer's instructions. Chromatographic separations were performed on a 2.1 × 150 mm chromatography column. The column was maintained at 43 °C, eluted with a mix of 99.9% of MassTrak AAA eluent A concentrate (8–10% acetonitrile, 4–6% formic acid, 84–88% ammonium acetate/water solution), and diluted at 10% in miliQ water and 0.1% of MassTrak AAA eluent B (≥95% acetonitrile, ≤5% acetic acid) with a flow rate of 0.4 ml/min. 1 μL of

deprotonized and derivatized sample was injected into the column with UV detection at 260 nm.

2.9. Statistical analysis

The results presented are expressed in mean value of N experiments ± S.EM, with N ≥ 3. Comparison of the data sets obtained from the different experiment conditions was performed with the Student *t* test. Differences were considered to be statistically significant when *P* values were ≤0.05.

The uptake and secretion of amino acid measured on cells expressing or deficient for c-Myc, Oct1 and KLF4, were compared with partial least squares analysis (PLS) for statistical discrimination.

3. Results

Bioenergetic reprogramming impacts the main pathways of energy production such as glycolysis and oxidative phosphorylation in most cancer cells. These two pathways are linked with amino acid consumption and synthesis, so that the follow-up of amino acid is intimately linked to energy metabolism, as illustrated in Fig. 1A. To study this link, we investigated the impact of three oncogenes on both energy and amino acid metabolism (Fig. 1B). The effect of each oncogene's expression inhibition on cellular proliferation was investigated in Fig. 2. As expected, c-Myc deficient cells had significantly reduced proliferation rate when compared to c-Myc proficient TGR-1 cells. The c-Myc re-expressing HOMYC cells had a higher proliferation rate as compared to the HO15 cells. Thus, we can conclude that

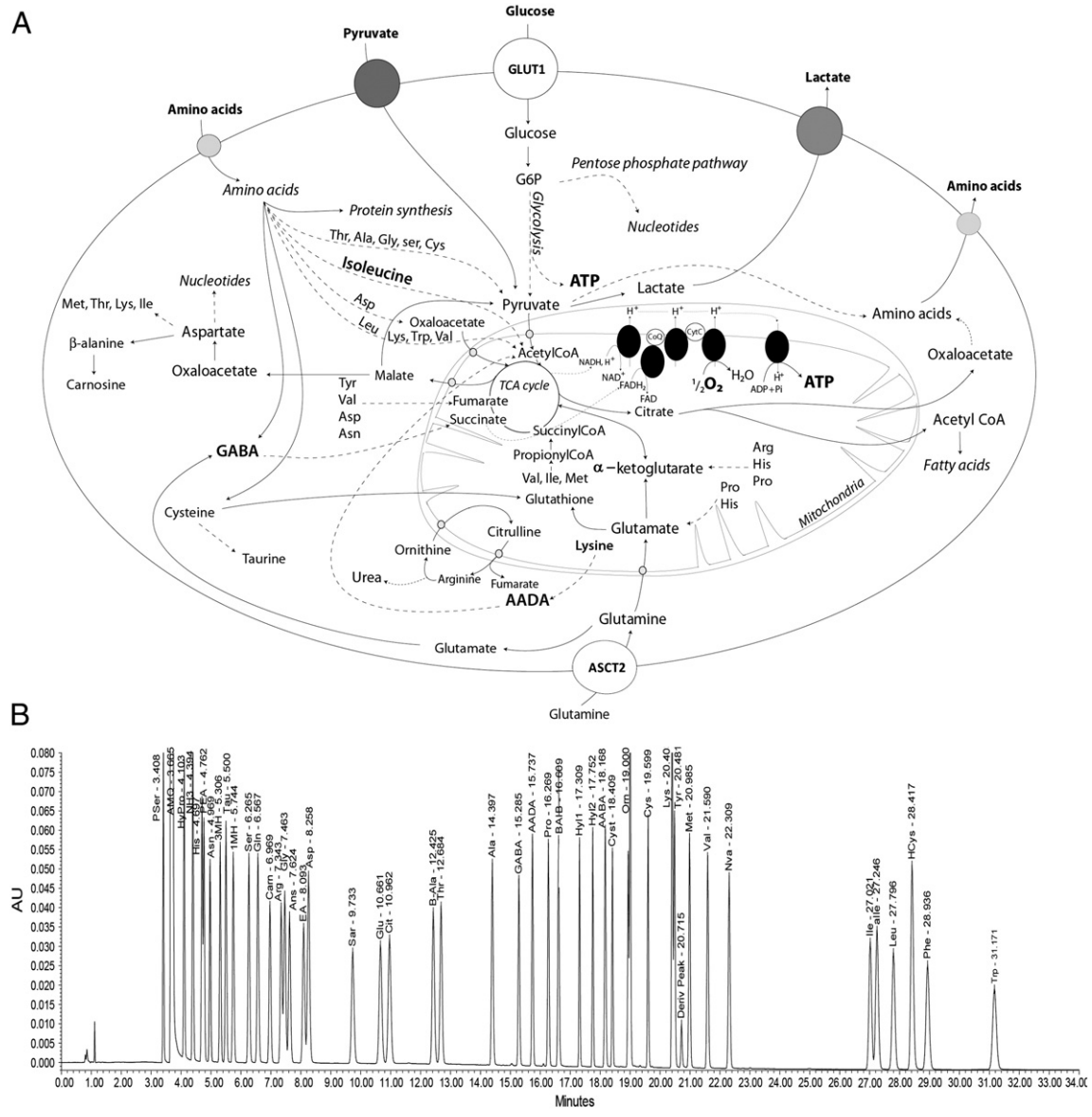

Fig. 1. Secretomics of fibroblasts in culture. The cell metabolism was measured at different aspects regarding extracellular metabolites in the wild-type and deficient cell lines (A). The amino acids uptake and release was quantified with the glucose and pyruvate consumptions, as well as the lactate secretion. The expression of glucose GLUT1 and glutamine transporters ASCT2 were also investigated. The glycolytic and mitochondrial contributions to ATP production were analyzed. And the oxygen consumption rates were determined. The chromatogram of the amino acids standard solution was obtained by UPLC (B). The specific retention times are indicated for each metabolite: Pser, phosphoserine; HyPro, hydroxyproline; NH3, Ammonia; PEA, phosphoethanolamine; Asn, Asparagine; 3MH, 3-methylhistidine; Tau, taurine; 1MH, 1-methylhistidine; Ser, serine; Gln, glutamine; Carn, carnosine; Arg, arginine; Gly, glycine; Ans, Anserine; EA, ethanolamine; Asp: Aspartic acid; Sar, sarcosine; Glu, glutamate; Cit, citrulline; B-ala, β-alanine; Thr, threonine; Ala, alanine; GABA, γ-amino-*N*-butyric acid; AADA, α-aminoadipic acid; Pro, proline; BAIB, β-aminoisobutyric acid; Hyl1, hydroxylysine 1; Hyl2, hydroxylysine 2; AABA, α-amino-*N*-butyric acid; Cyst, Cystathionine; Orn, Ornithine; Cys, cystine; Lys, lysine; Tyr, tyrosine; Met, methionine; Val, valine; Nva, norvaline; Ile, isoleucine; Alle, *allo*-isoleucine; Leu, leucine; Hcys, homocystine; Phe, phenylalanine; Trp, tryptophan. Norvaline was added in the different media samples as an internal standard.

inhibition of c-Myc expression decreased cellular proliferation (Fig. 2A) as shown in previous studies [10,11]. We noticed that proliferation rate of KLF4 $^{-/-}$ was marginally higher compared to the KLF4 wild-type cells after 4 days of culture (Fig. 2B). On the other hand, no significant difference was observed for the proliferation rate between wild-type and Oct1$^{-/-}$ MEFs (Fig. 2C).

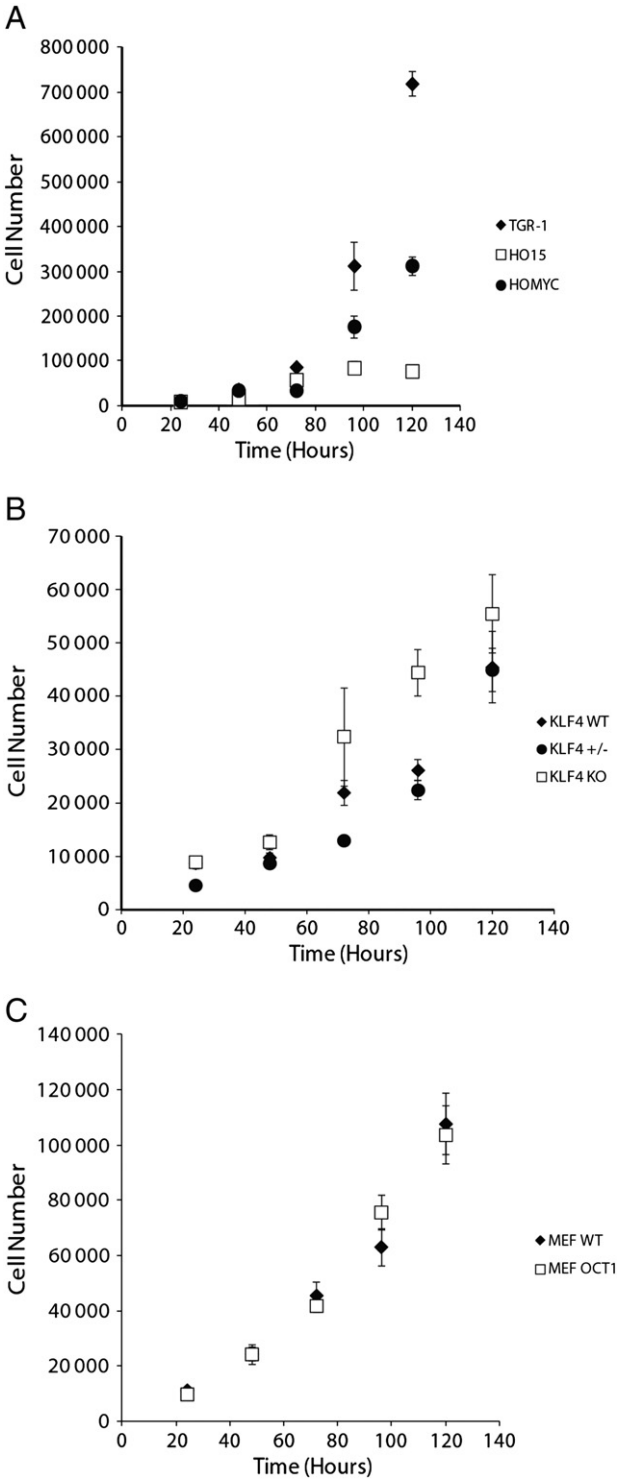

Fig. 2. c-Myc and KLF4 expression inhibition differentially regulates cell proliferation. The effect of c-Myc (A), KLF4 (B) and Oct1 (C) expression on cell proliferation was measured on days 1, 2, 3, 4, and 5. The numbers of live cells were counted using trypan blue (0.2%) dye exclusion method for each time point. The growth curve for each cell type is combination of three independent experiments performed in triplicate. Here, cell numbers are shown as mean ± S.E.M.

3.1. Effect of c-Myc on metabolomics and bioenergetics

We first analyzed c-Myc induced changes in cell metabolism. We compared the glucose uptake in c-Myc proficient fibroblasts (TGR-1 and HOMYC) and c-Myc deficient cells (HO15) over 24 h of growth in high glucose DMEM. c-Myc deficient HO15 cells showed a twice higher glucose consumption compared to the c-Myc expressing TGR-1 (0.0967 ± 0.0132 versus 0.0697 ± 0.00437 μmol/μg of protein, $P<0.05$) or to the HOMYC cells (0.0766 ± 0.0214 μmol/μg of protein) (Fig. 3A). These results indicate that c-Myc negatively controls glucose consumption as previously shown in other cell types [12,13]. High glycolysis is typically associated with lactic acidosis, so we measured the concentration of excreted lactate to verify the potential occurrence of the Warbug effect. As expected, the amount of lactate secreted by the c-Myc deficient HO15 cells was higher as compared to TGR-1 cells (0.0134 ± 0.00099 versus 0.0093 ± 0.00027 μmol/μg of protein, $P<0.001$). This metabolic disturbance was rescued by the recovery of c-Myc activity as the quantity of lactate released in the incubation medium by the c-Myc re-expressing HOMYC cells was lower than in the HO15 cells with $P=0.0001$ (Fig. 3B). To investigate the mechanisms underlying the non-complete oxidation of glucose, we evaluated the capacity of the cells to oxidize pyruvate via oxidative phosphorylation. We observed a lower pyruvate uptake (Fig. 3C) in HO15 cells compared to the TGR-1 cells (0.0041 ± 0.00033 and 0.0066 ± 0.00061 μmol/μg of protein respectively, $P<0.01$). Taken together, these results indicate that c-Myc deficient cells present the Warburg effect and derive energy primarily from high glycolysis rather than OXPHOS.

To evaluate the impact of c-Myc inactivation on mitochondrial function, we measured the oxygen consumption rate (OCR) in HO15 cells and controls using the XF24 Seahorse analyzer. As seen in Fig. 3D, the baseline OCR measured in HO15 cells was significantly lower than in c-Myc proficient TGR-1 cells (27.67 ± 4.42 pmol/min versus 67 ± 12.72 respectively, $P<0.05$). To assess the full capacity of the respiratory chain, we used 2.5 μM FCCP to uncouple OXPHOS. As expected, uncoupled respiration was strongly reduced in the HO15 cells (39.89 ± 5.18 pmol/min) as compared to the TGR-1 cells (103.71 ± 21.39 pmol/min). Inhibition of the mitochondrial phosphorylation system with 2 μg/mL oligomycin allowed to calculate the respiratory control ratio (RCR) which gives a measure of the mitochondrial respiration for ATP synthesis. As seen in Fig. 3E, HO15 cells presented with a low RCR value (2.23 ± 0.28) as compared to TGR-1 cells (3.98 ± 0.66). Lastly, the rescue of c-Myc expression in HOMYC cells reset the coupling ratio to normal values (4.30 ± 0.96, $P<0.05$ versus the c-Myc deficient cells RCR of 2.23). However, c-Myc reactivation in HO15 cells could not recover the uncoupled OCR, suggesting that irreversible changes had occurred in the OXPHOS system of c-Myc deficient cells.

To fully characterize the bioenergetic changes induced by c-Myc deficiency, we measured the steady-state ATP production and determined the relative contribution of OXPHOS to cellular ATP synthesis by performing the inhibition of the F1F0-ATPsynthase with oligomycin as previously described [14]. As seen in Fig. 3F, the ATP production in presence of oligomycin was unchanged in HO15 cells in (100.74 ± 2.14% of the untreated HO15), as compared to the TGR-1 controls where a reduction was observed (86.43 ± 2.89% of the untreated TGR-1).

To understand the c-Myc deficiency induced mitochondrial changes, we measured the protein content of several respiratory chain complexes sub-units (Fig. 4). We noticed a lower expression level of CI20 in HO15 and HOMYC than in TGR-1 cells. However, the c-Myc deficient cells presented no significant difference in the other OXPHOS protein expression level when compared to the both c-Myc expressing cells. The higher glucose uptake measured in the c-Myc deficient cells was explained by a higher expression of GLUT1 in HO15 cells as compared to TGR-1 and HOMYC (Fig. 4). Furthermore,

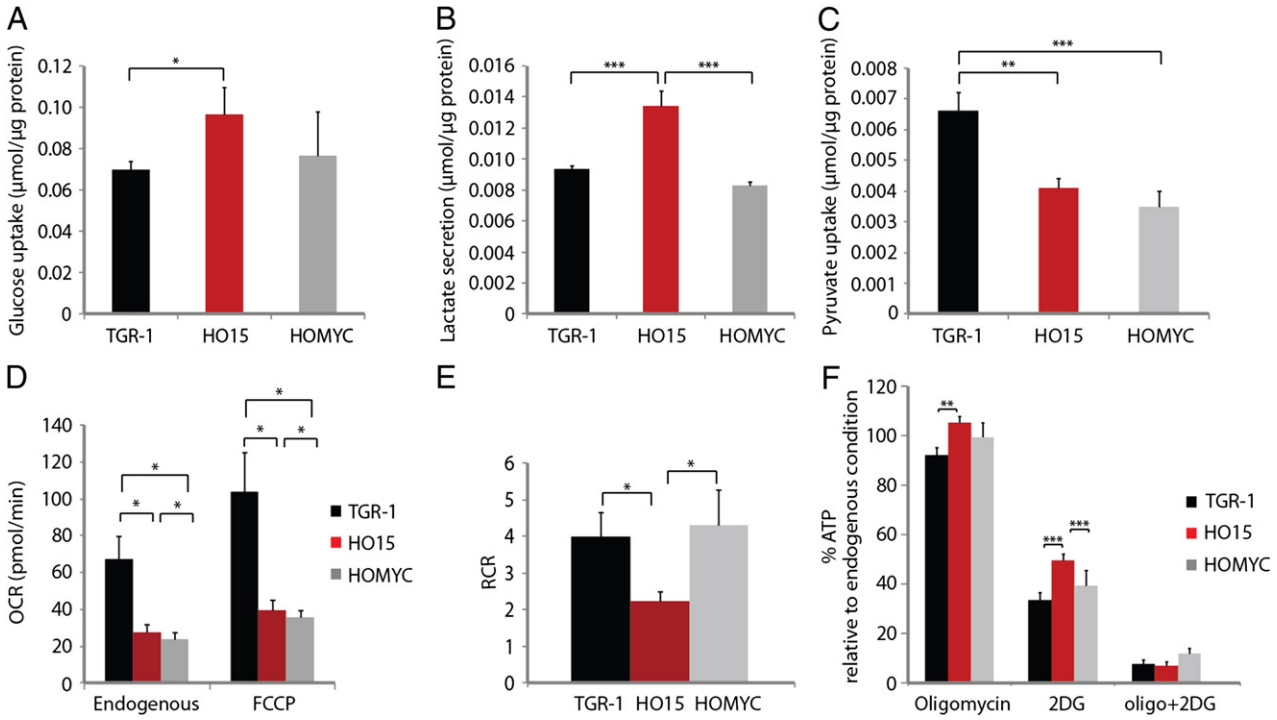

Fig. 3. Effect of c-Myc expression on the glycolytic substrates consumption, mitochondrial respiration and energy production. The glucose consumption (A), the lactate secretion (B) and the pyruvate uptake (C) were measured in rat fibroblasts. Each metabolite was measured after 24 h of incubation in high glucose DMEM (25 mM glucose) as growth media. The corresponding cell pellets were used for quantifying the protein content for normalization. The results are expressed in µmol/µg protein as mean ± S.E.M for the glucose, lactate and pyruvate content (*, $P<0.05$; **, $P<0.01$ and ***, $P<0.001$). The oxygen consumption rate (OCR) has been measured in high glucose DMEM (HG, 25 mM glucose, 1 mM pyruvate and 4 mM glutamine) under endogenous condition or in the presence of FCCP (2.5 µM) on the TGR-1, HO15 and HOMYC cells (D) The OCR values expressed in pmol/min represent means ± S.E.M (*, $P<0.05$). The RCR has also been determined by calculating the ratio of baseline OCR on the respiration in presence of 2 µg/ml oligomycin (E). Then the quantity of ATP produced by TGR-1, HO15 and HOMYC cells (F) were determined in DMEM HG medium in presence of oligomycin (2.5 µg/µl) and/or 2DG (100 mM). Data is expressed for each cell type in percent of ATP content without inhibitor as the mean ± S.E.M (*, $P<0.05$; **, $P<0.01$ and ***, $P<0.001$).

the lower expression level of PKM2 in c-Myc deficient cells than in TGR-1 and HOMYC cells confirmed the enhancement of glycolysis in c-Myc expressing cells.

To study the impact of c-Myc on amino acids metabolism, we analyzed the uptake/secretion of 40 amino acids in these cells after 24 h of incubation in high glucose DMEM (Fig. 5A and B). We noticed that branched-chain amino acids (BCAA) uptake such as Isoleucine, leucine and valine, were reduced (greater than two folds, $P<0.05$) in c-Myc deficient HO15 cells, as compared to c-Myc proficient TGR-1 cells. MFP also revealed an increase in the uptake of the ketogenic amino acid lysine in HO15 cells as compared to TGR-1 and HOMYC cells (2.72 and 1.98 as fold change, respectively, $P<0.05$). We further observed significant change in the level of taurine, which was secreted by the cells expressing c-Myc (TGR-1 and HOMYC) but consumed from the medium by c-Myc deficient HO15 cells. There was also a significant increase in alanine secretion in the c-Myc proficient cells (1.61 and 1.56 fold change in TGR-1 cells and HOMYC respectively, $P<0.05$, relative to HO15 cells). Interestingly, we detected that the uptake flux of citrulline, an amino acid involved in urea cycle, was significantly upregulated in HO15 cells compared to that in HOMYC. Furthermore, we noticed that the uptake flux of 4-aminobutyrate (GABA), a neurotransmitter, was also significantly increased in HO15 cells as compared to TGR-1 and HOMYC cells. Lastly, the secretion of ethanolamine (EA), an amino acid involved in phospholipids synthesis, was dramatically increased (greater than eight fold) in HO15 cells compared to TGR-1. The cystine uptake flux was remarkably increased and its precursor cystathionine secretion was reduced in HO15 cells compared to TGR-1 cells. These findings indicate that c-Myc not only modulates glutamine metabolism [15] but also impacts the catabolism and the synthesis of other amino acids. We illustrated the simplified amino acids secretomics profile of c-Myc deficient cells (changes greater than 1.5) in supplemental data.

3.2. Effect of KLF4 on metabolomics and bioenergetics

To examine the influence KLF4 on cell metabolism, we performed the same approach as for c-Myc. Both glucose uptake and lactate secretion were significantly higher in KLF4$^{-/-}$ cells than in the KLF4 wild-type (factor of 3.81 for the glucose consumption and of 1.36 for the lactate secretion) (Fig. 6A and B). Thus, KLF4 expression seems to be inversely correlated with the glycolytic phenotype, as for c-Myc. The decline in KLF4 expression during the exponential phase of proliferation could explain the enhancement of glycolysis phenotype obtained with the KLF4$^{-/-}$ cells. This profile is in accordance with the Warburg effect observed in highly proliferative cancer cells. Lastly, we observed a lower pyruvate uptake (Fig. 6C) in KLF4$^{-/-}$ cells compared to the KLF4 $^{+/-}$ cells.

To investigate the impact of KLF4 on mitochondrial metabolism, we measured the OCR (Fig. 6D). Interestingly, KLF4 wild-type, KLF4$^{+/-}$ and KLF4$^{-/-}$ cells had similar endogenous respiration (around 109.20 ± 6.71 pmol/min for the wild-type, 128.44 ± 26.06 for the KLF4$^{+/-}$ and 101 ± 5.28 pmol/min for the KLF4$^{-/-}$ cells). Furthermore, the inhibition of KLF4 expression had no impact on the RCR (2.59 ± 0.36, 2.85 ± 0.25 and 2.36 ± 0.17 for the KLF4 wild-type, KLF4$^{+/-}$ and, KLF4$^{-/-}$ respectively), indicating that KLF4 has no regulatory effect on mitochondrial respiration (Fig. 6E). We next assessed the impact of KLF4 on ATP production (Fig. 6F). The inhibition of ATP production with 2-deoxy-D-glucose (2DG) reflected the contribution of glycolysis. To verify that the changes induced by 2DG were not related to the possible induction of cell death, we quantified the amount of live and dead cells in the experimental conditions used for ATP measurements (supplemental Fig. 1). We noticed no activation of cell death so that the observed decrease of ATP content triggered by 100 mM 2DG was not the consequence of cell death. In addition, the ATP content measured in the presence of 2DG indicated

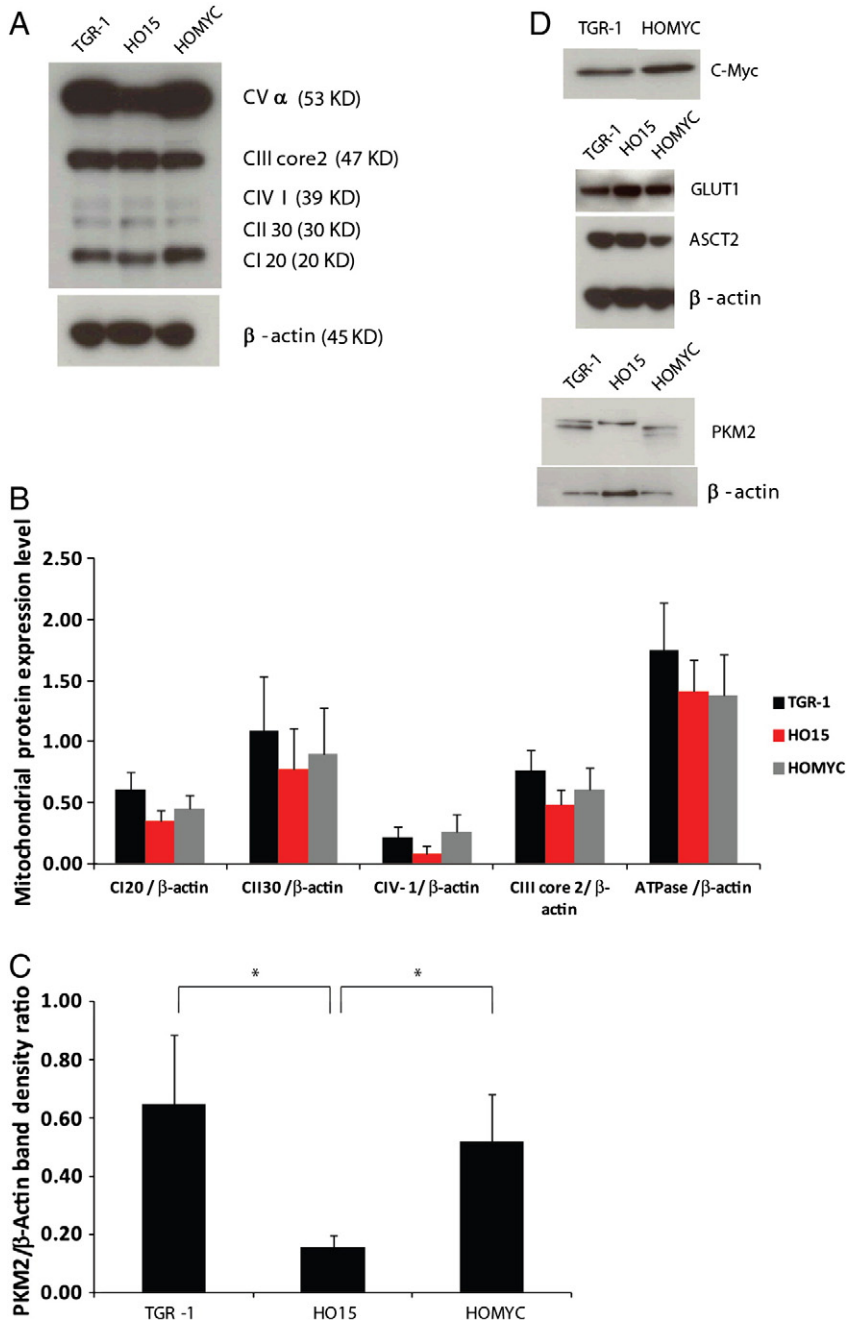

Fig. 4. Expression of mitochondrial protein in TGR-1, HO15 and HOMYC cells. The OXPHOS complexes and glycolytic enzyme PKM2 expression level were quantified by western blot on cell lysate prepared from TGR-1, HO15 and HOMYC (A). The results are expressed in band density ratios of mitochondrial (B) or glycolytic protein PKM2 (C) on β-actin as mean ± SD (*, $P<0.05$). The expression of c-Myc, GLUT1 and ASCT2 expression level were quantified by western blot, on cell lysate of TGR-1, HO15 and HOMYC cells (D).

that glycolysis provided energy to a greater extend in KLF4 $^{+/-}$ and KLF4 $^{-/-}$ when compared to the KLF4 $^{+/+}$ cells (39.20 ± 3.39% for the KLF4$^{-/-}$, 37.57 ± 2.12% for the KLF4$^{+/-}$ and 45.15 ± 2.78% for the KLF4 wild-type). The treatment of these cells with oligomycin confirmed these findings as this drug had minor effect on the ATP levels (92.30 ± 3.54 for KLF4$^{+/+}$, 97.79 ± 10.09% for the KLF4$^{+/-}$ and 93.36 ± 5.49% for the KLF4$^{-/-}$ cells). These results also revealed that KLF4 had little impact on the contribution of mitochondria to cellular ATP synthesis.

To investigate the role of KLF4 in both the uptake and release of amino acid, we performed UPLC analysis of the spent media after 24 h of incubation. The detailed amino acid amounts are shown in supplemental Table 2. The uptake of valine was significantly higher in KLF4 WT cells compared to that in KLF4$^{-/-}$ cells (Fig. 7). As was observed with the measurement of glycolysis, we noticed a significant increase (thirty-eight folds increase) in secretion of glucogenic amino acid aspartate in KLF4 WT cells compared to KLF4$^{-/-}$ cells. There was a remarkable reduction in glutamine uptake in KLF4 WT cells compared to that in KLF4$^{-/-}$ cells. Moreover, the uptake of phenylalanine and tyrosine were increased in the KLF4$^{-/-}$ cells compared with the wild-type (1.99 fold change of phenylalanine; 1.66 fold change of tyrosine). These amino acids are involved in the formation of fumarate which serves to fuel the Krebs cycle and subsequent respiratory chain. The secretion of ethanolamine, sarcosine, and β-alanine were significantly increased in KLF4 WT cells compared to that in KLF4$^{-/-}$ cells. The uptake of ornithine, citrulline, and 1-methyl histidine, were increased in KLF4 WT cells compared to that in KLF4$^{-/-}$ cells. We observed that uptake of lysine, a ketogenic

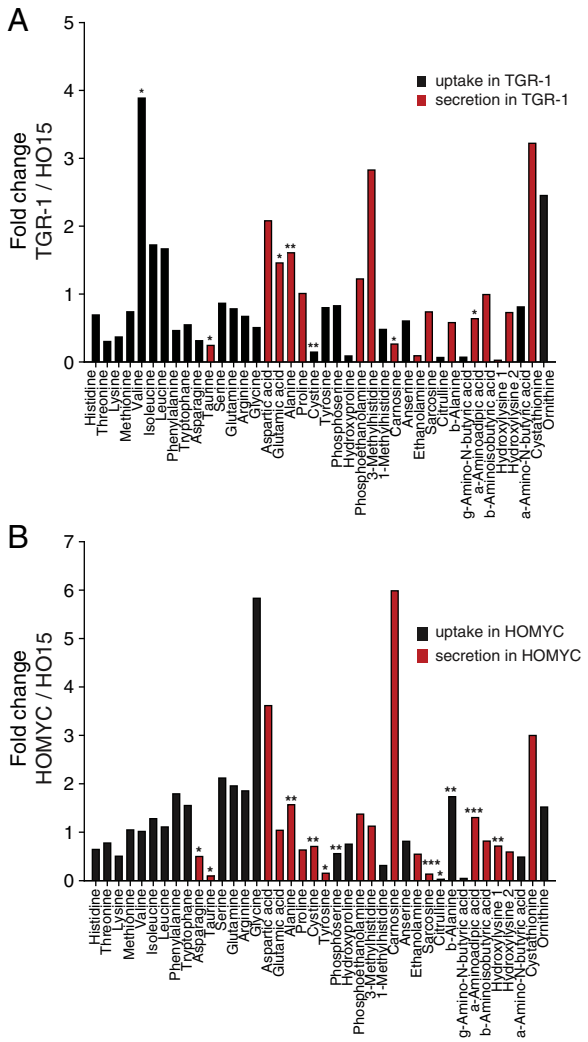

Fig. 5. Effect of c-Myc expression on the metabolomics. The amino acid secretion and uptake were measured on the cells c-Myc deficient (HO15) and the one expressing c-Myc (TGR-1 and HOMYC) after 24 hour incubation. The results are expressed in fold changes relative to HO15 for c-Myc proficient TGR-1 (A) and HOMYC (B) (*, $P<0.05$; **, $P<0.01$ and $P<0.001$).

amino acid was upregulated in KLF4$^{-/-}$ cells compared to that in wild-type cells. Notably, secretion of amino acids involved in urea cycle, such as asparagine and arginine; formation of α-ketoglutarate (proline, arginine and histidine), formation of pyruvate (alanine and glycine), and formation of TCA cycle substrates (hydroxylysine 1) was upregulated in KLF4$^{-/-}$ cells compared to that in wild-type cells. We observed an inversion in serine and cystine contents. They were consumed in KLF4 deficient cells but secreted in the wild-type. We found a similar behavior with hydroxyproline, which was secreted in the wild-type cells (0.00011 ± 0.000021 μmol/μg protein) in contrast to KLF4$^{-/-}$ cells where it was uptaken (0.000125 ± 0.0000495 μmol/μg protein). Interestingly, secretion of α-aminoadipic acid (amino acid involved in synthesis of lysine and acetyl-CoA), β-aminoisobutyric acid (product of thymine metabolism), and phosphoethanolamine (involved in phospholipid metabolism) were remarkably increased in KLF4$^{-/-}$ cells compared to the wild-type cells. KLF4 seems to be involved in antioxidant pathways with the anserine uptake and the carnosine secretion increased in KLF4$^{-/-}$ cells as compared to wild-type cells. These observations suggest that KLF4 is not only involved in inhibiting glycolysis but also regulates phospholipid metabolism, nitrogen balance, and DNA and RNA metabolism.

3.3. Effect of Oct1 on metabolomics and bioenergetics

To assess the impact of Oct1 deficiency on energy metabolism, we analyzed glucose and pyruvate uptake as well as lactate secretion in wild-type and Oct1$^{-/-}$ MEFs. We observed that the inhibition of Oct1 expression induced a significant decrease in glucose consumption (0.135 ± 0.042 μmol/μg of protein) as compared to the wild-type MEFs (0.283 ± 0.051 μmol/μg of protein, $P<0.05$) in high glucose medium (Fig. 8A). Accordingly, the amount of lactate released by Oct1$^{-/-}$ cells was lower than their wild type counterparts (factor 1.9) in high glucose medium (Fig. 8B). Oct1$^{-/-}$ cells displayed a poor utilization of pyruvate suggesting an involvement of Oct1 in the regulation of pyruvate uptake and/or oxidation (0.015 ± 0.0036 in MEF wild-type and 0.0045 ± 0.00135 μmol/μg protein in the MEF Oct1 $^{-/-}$ (Fig. 8C).

To assess the possible role of Oct1 in the regulation of mitochondrial respiration, we measured the baseline OCR and RCR. There was no significant difference between the baseline OCR in MEF wild-type (104.25 ± 10.65 pmol/min) and the MEF Oct1 deficient cells (114.77 ± 9.70 pmol/min) (Fig. 8D). However, the inhibition of Oct1 expression provided a better RCR (3.16 ± 0.23 for the MEF Oct1$^{-/-}$ and 2.41 ± 0.20 for the wild-type) (Fig. 8E). This coupling ratio is explained by the energy production process. As seen in Fig. 8F, the Oct1$^{-/-}$ MEFs cells exhibited a lower ATP content than ($90 \pm 3.88\%$) the wild-type MEF cells ($101.74 \pm 5.71\%$) in the presence of oligomycin. The increase in ATP production observed after 1 h of incubation in the presence of oligomycin suggested that the cells were able to stimulate glycolysis in order to compensate for the inhibition of mitochondrial ATP synthesis. This process might be considered as compensatory ATP generation [16]. However, the glycolysis inhibition by 2DG indicated that the capacity to generate ATP through glycolysis was more important in Oct1 $^{-/-}$ MEF cells than in wild-type cells ($36.61 \pm 2.58\%$ and $32.06 \pm 2.78\%$ respectively, $P<0.01$).

We pursued the MFP approach in order to obtain the detailed uptake/secretion values (supplemental Table 3). The uptake of BCAAs was significantly increased in wild-type Oct1 cells compared to Oct1 deficient cells (Fig. 9). Interestingly, we observed significant increase in the uptake of aspartate and of hydroxylysine, two amino acids involved in the formation of TCA cycle substrates in wild-type Oct1 cells compared to that in Oct1$^{-/-}$ cells. Furthermore, the uptake of γ-amino-*N*-butyric acid was increased in Oct1$^{-/-}$ cells compared to that in the wild-types cells. However, secretions of lysine, alanine, phosphoethanolamine, β-alanine, α-amino adipic acid, β-amino isobutyric acid and ornithine were significantly higher in Oct1 WT cells compared to that in Oct1$^{-/-}$ cells. This indicates that Oct1 is involved in upregulation of secretion of these amino acids. Oct1 inhibition induced a decrease in the uptake of all essential amino acids except in valine with fold changes between 0.43 and 0.60 compared to the wild-type MEFs (Fig. 9). The uptake of histidine, threonine, methionine, phenylalanine, tryptophan, taurine, carnosine, anserine, ethanolamine, citrulline, asparagine, serine, glutamine, arginine and tyrosine and the secretion of alanine were significantly increased in the wild-type Oct1 cells compared to that in Oct1 deficient cells. Taken together, our metabolic profile data suggest that Oct1 promotes protein synthesis and stimulates the TCA cycle. The specific MFP profile of Oct1$^{-/-}$ cells is given in supplemental Fig. 2.

3.4. Oncosecretomics and biomarkers

Data on 12 to 15 samples of measurements for each of the forty amino acids for each oncogene were analyzed via partial least squares discriminant analysis to determine the groups of amino acids that are responsible for best separating the wild-type and deficient cells for c-Myc, Oct1 or even KLF4. All samples with over 50% missing measurements were removed, the data was standardized and remaining missing values were imputed via five-nearest neighbors [17]. For

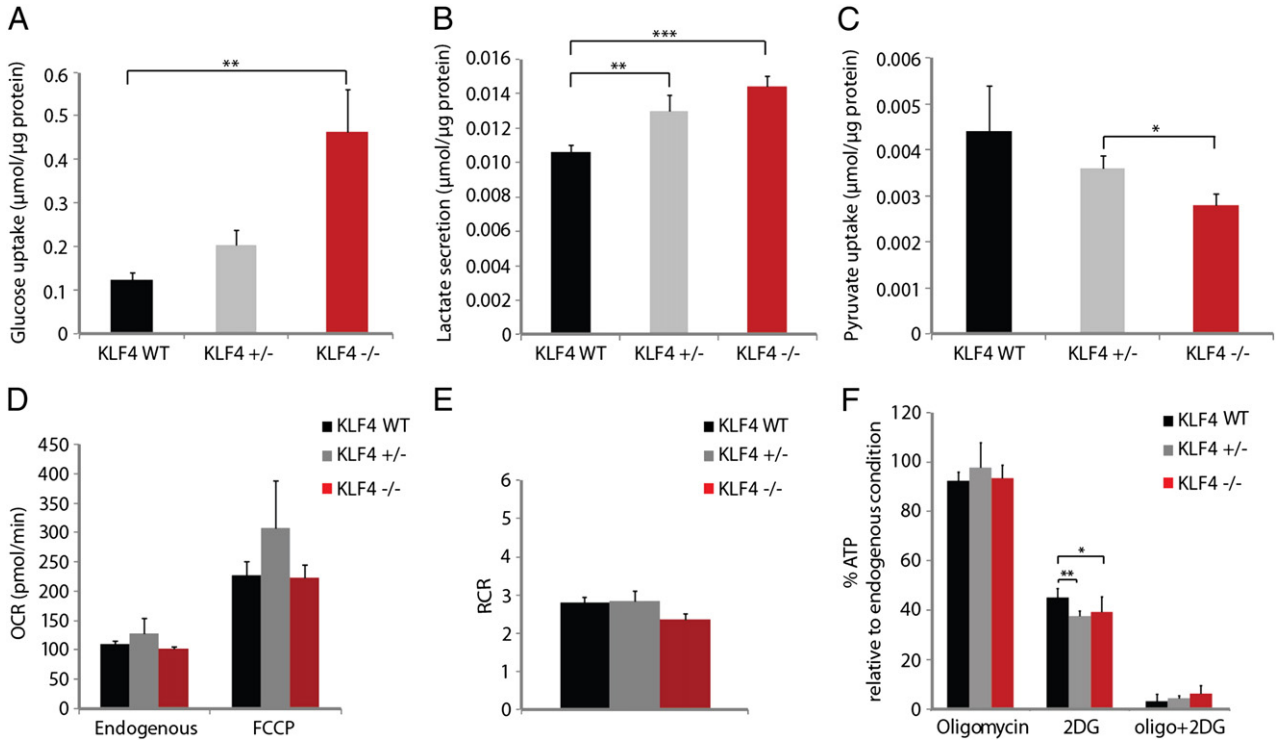

Fig. 6. Effect of KLF4 expression on glycolytic metabolites, mitochondrial respiration and energy production. The glucose consumption (A), the lactate secretion (B) and the pyruvate uptake (C) were measured in MEFs. Each metabolite was measured after 24 h of incubation in high glucose DMEM (25 mM glucose) as growth media. The corresponding cell pellets were used for quantifying the protein content for normalization. The results are expressed in µmol/µg protein as mean ± S.E.M for the glucose, lactate and pyruvate content (*, $P<0.05$; **, $P<0.01$ and ***, $P<0.001$). The oxygen consumption rate (OCR) has been measured in high glucose DMEM (HG, 25 mM glucose, 1 mM pyruvate and 4 mM glutamine) under endogenous condition or in the presence of FCCP (2.5 µM) on the KLF4 wild-type, KLF4 $^{+/-}$ and KLF4 $^{-/-}$ cells (D). The OCR values expressed in pmol/min represent means ± S.E.M (*, $P<0.05$). The RCR has also been determined (E). Then, the quantity of ATP produced by the wild-type, KLF4 $^{+/-}$ and KLF4 $^{-/-}$ cells (F) were determined in DMEM HG medium in presence of oligomycin (2.5 µg/µl) and/or 2DG (100 mM). Data is expressed for each cell type in percent of ATP content without inhibitor as the mean ± S.E.M (*, $P<0.05$; **, $P<0.01$ and ***, $P<0.001$).

each of the pairs of comparison factors, partial least squares discriminant analysis was performed [18]. Results of this method forclassifying samples between wild-type and knockout are given in supplemental Table 4. Training misclassification errors are given using all the samples and testing errors are estimated by employing leave one out cross-validation. In Fig. 10, scatterplots of the first two PLS component loadings are given illustrating the clusters of amino acids that contribute to classifying between wild-type and c-Myc,

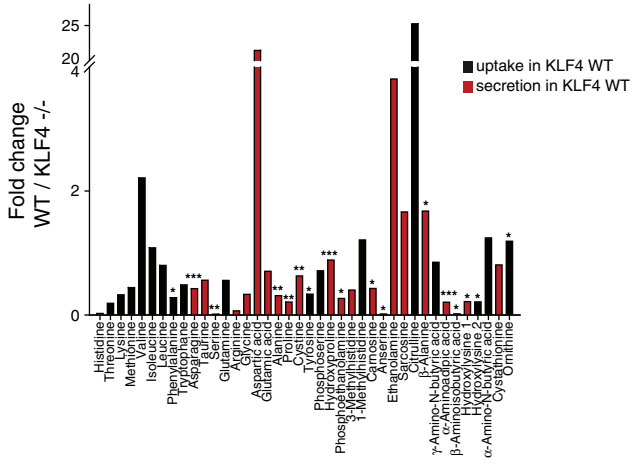

Fig. 7. Effect of KLF4 expression on metabolomics. The secretion of essentials, nonessentials and secondary amino acids were measured on MEF cells after 24 hour incubation in growth media. The amino acid secretion and uptake are expressed in fold changes of the wild-type relative to KLF4 $^{-/-}$ (A) (*, $P<0.05$; **, $P<0.01$ and $P<0.001$).

KLF4 and Oct1 deficient cells. Groups of amino acids from these scatterplots reveal significant patterns that well separate the two classes. Thus, among all the amino acids identified, isoleucine could be considered as a biomarker related to c-Myc expression. Isoleucine is a precursor of acetyl-CoA and succinyl-CoA, intermediary of the TCA cycle. Importantly, the increased isoleucine uptake induced by c-Myc could explain the increase in RCR observed in TGR-1 and HOMYC cells. For KLF4, α-aminoadipic acid is the metabolite that distinguishes the wild-type and deficient cells. As mentioned previously, AADA can lead to the production of acetyl-CoA which seems to induce fatty acid synthesis instead of providing substrates for mitochondria. Lastly, we found that γ-Amino-*N*-butyric acid (GABA) flux is correlated with Oct1 expression. The increased consumption of GABA, a precursor of succinate, stimulates the TCA cycle, and thus may explain the better efficiency of mitochondrial respiration for ATP production in the MEF Oct1$^{-/-}$ compared to the wild-type as observed in our results.

4. Discussion

The fundamental objective of this work was to assess in parallel the bioenergetic and the secretomic impact of three oncogenes in order to evaluate the predictive potential of metabolic footprinting. The secondary aim was to reveal patterns of interest for cancer diagnosis and follow-up. The three oncogenes selected, c-Myc, KLF4 and Oct1 were chosen for their recognized implication in carcinogenesis but also for their recently described participation in cell differentiation and the generation of induced pluripotent stem cells [19,20].

Previous biochemical studies indicate that c-Myc is not only overexpressed in several tumors but also that its overall impact on bioenergetics is complex. Indeed, c-Myc can activate the expression

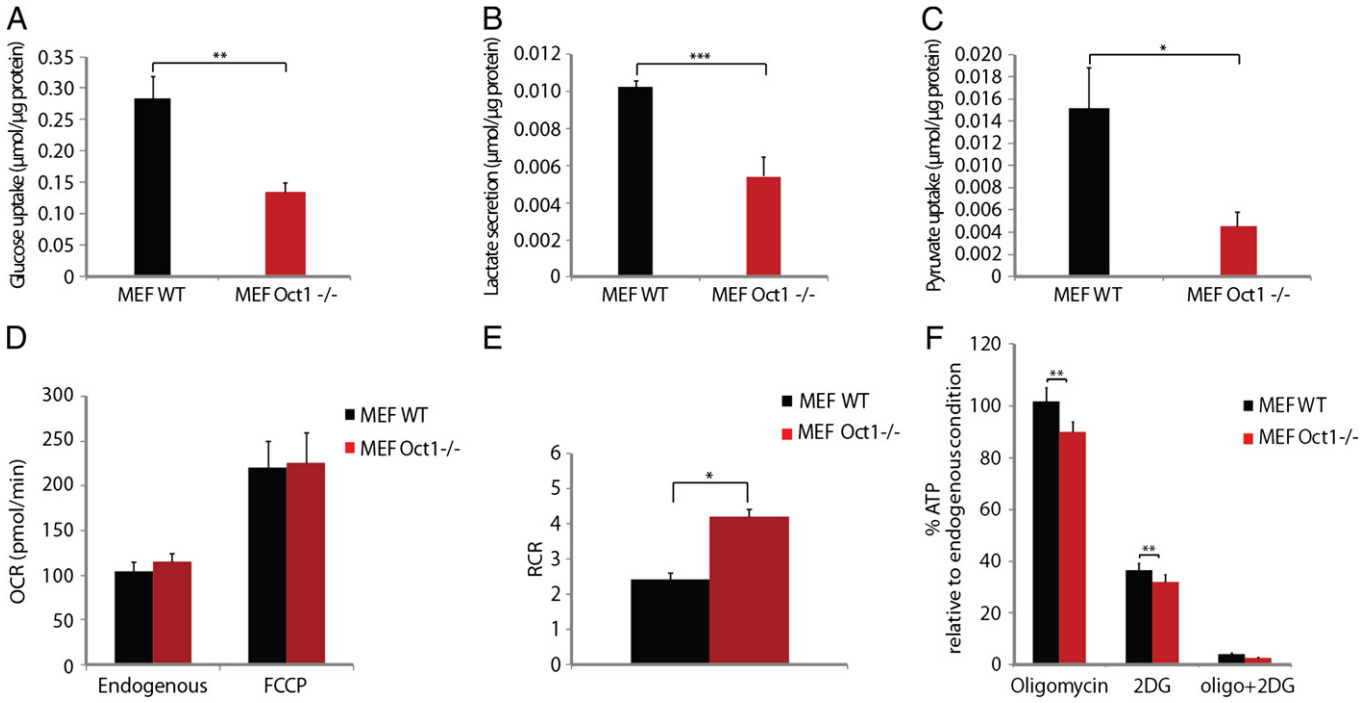

Fig. 8. Effect of Oct1 expression on metabolomic, mitochondrial respiration and energy production. The glucose consumption (A), the lactate secretion (B) and the pyruvate uptake (C) were measured in MEFs. Each metabolite was measured after 24 h of incubation of the MEF Oct1 wild-type and MEF Oct1 $^{-/-}$ cells, in high glucose DMEM (25 mM glucose) as growth media. The corresponding cell pellets were used the protein content measurement for normalization. The results are expressed in µmol/µg protein as mean ± S.E.M for the glucose, lactate and pyruvate contents (*, $P<0.05$; **, $P<0.01$ and ***, $P<0.001$). The oxygen consumption rate (OCR) has been measured in high glucose DMEM under endogenous condition or in the presence of FCCP (2.5 µM) on the MEF Oct1 wild-type and Oct1 $^{-/-}$ cells (D). The OCR values expressed in pmol/min represent means ± S.E.M (*, $P<0.05$). The RCR has also been determined (E). Then, the quantity of ATP produced by the wild-type and Oct1 $^{-/-}$ cells (F) were determined in DMEM HG medium in presence of oligomycin (2.5 µg/µl) and/or 2DG (100 mM). Data is expressed for each cell type in percent of ATP content without inhibitor as the mean ± S.E.M (*, $P<0.05$; **, $P<0.01$ and ***, $P<0.001$).

of key glycolytic enzymes and also stimulate the uptake and the oxidation of glutamine by the OXPHOS system [21,22]. c-Myc was further shown to stimulate mitochondrial biogenesis [23] and thus could be considered as a master regulator of energy metabolism. We first characterized the c-Myc induced changes in cell metabolism by measuring the uptake of glucose and pyruvate concomitantly with lactate secretion. The glucose uptake and the lactate secretion are the two parameters, which define the Warburg effect [24,25]. In our study, the high glucose uptake observed in c-Myc deficient cells is consistent with the bioenergetic remodeling described in induced pluripotent stem cells (iPSC) where c-Myc expression was inhibited [12] and in cMycCHO cells expressing c-Myc, characterized by a glucose consumption and a lactate secretion decreased [13]. The measurements performed led us initially to the conclusion that c-Myc deficiency induces the Warburg effect. It is known that c-Myc induces the stimulation of glycolysis by increasing the expression of different enzymes, including glucose transporter (GLUT1), LDH-A [21] and pyruvate kinase M2 (PKM2) which is a strongly controlling step of glycolysis (see [26] for review). To verify this point, we analyzed PKM2 expression by western blot and found a higher content of this protein in TGR-1 and HOMYC cells (active c-Myc) as compared to HO15 cells (inactive c-Myc). Furthermore, we specified some features of c-Myc activation as we found that in addition to the above mentioned effect of c-Myc on glycolysis, this oncogene stimulates mitochondrial ATP production and thereby enhances the respiratory coupling ratio. Accordingly, our secretomic analysis shows that the observed higher efficiency of the OXPHOS system in c-Myc expressing cells might result from the increased consumption of isoleucine which is a precursor of various anaplerotic substrates [27]. Likewise, lysine and leucine can also be converted to acetoacetyl-CoA and then enter the TCA cycle through acetyl-CoA [28,29]. Our findings might suggest that c-Myc's pro-oxidative effect is not restricted to glutamine [15] and could also concern lysine and leucine, both of which can generate acetyl-coA and enter the Krebs cycle for complete catabolism. Furthermore, a recent study showed that supplementation of three BCAAs: leucine, isoleucine, and valine supported mitochondrial biogenesis in cardiac and skeletal muscle [30] and c-Myc expression has been previously associated with increased mitochondrial biogenesis [23]. Lastly, according to the profile generated with the MFP approach, we provided evidence that c-Myc proficient cells had higher taurine secretion compared to c-Myc deficient cells. This metabolite has been implicated in the regulation of cell volume and was found to be upregulated in

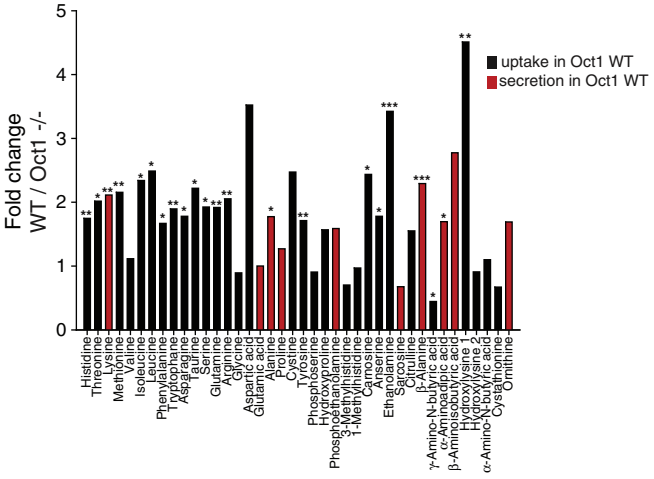

Fig. 9. Effect of Oct1 expression on metabolomic. The amino acid secretion and uptake were quantified on MEF wild-type and Oct1$^{-/-}$ after 24 h of incubation. The results are expressed in fold changes of the wild-type relative to Oct1 $^{-/-}$ (A) (*, $P<0.05$; **, $P<0.01$ and $P<0.001$).

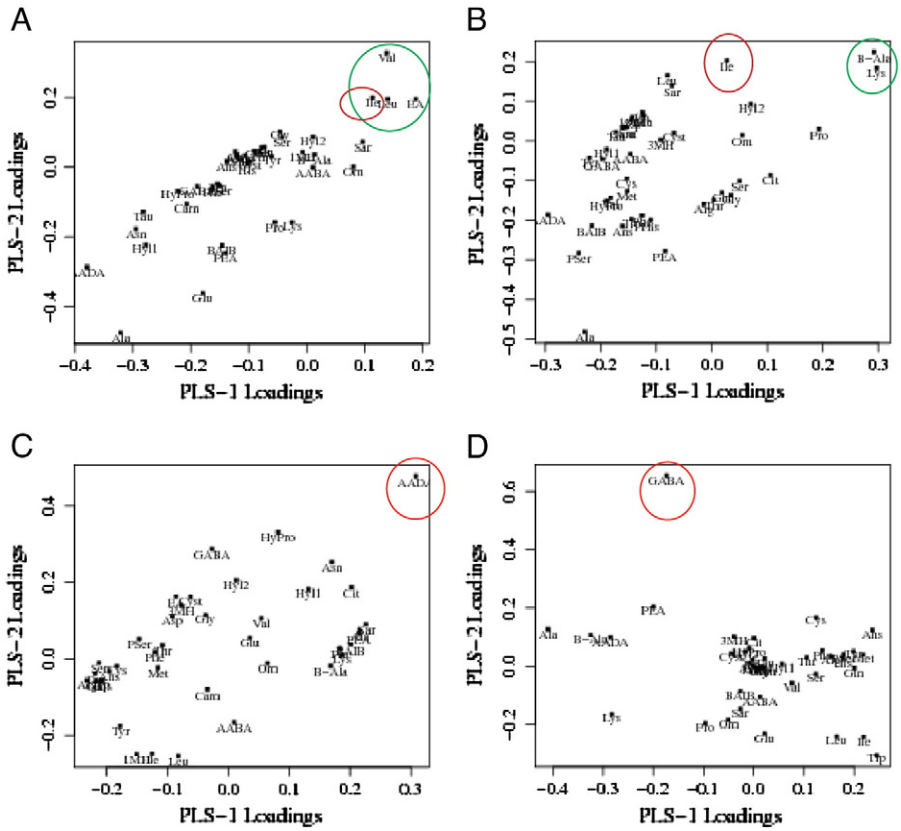

Fig. 10. Partial least squares discriminant scatterplots of amino acids related to oncogene expression. The key metabolites that discriminate TGR-1 (A) or HOMYC (B) with HO15 cells are circled in green. But the amino acids attributed to c-Myc expression, as well as the biomarkers revealed when comparing KLF4 (C) and Oct1 (D) deficient cells with their respective control, are circled in red.

squamous cell carcinoma [31]. We observed a higher alanine uptake in TGR-1 and HOMYC cells compared to HO15 cells. The alanine uptake can lead to the production of pyruvate and provide substrates such as NADH for the OXPHOS system. Hence, c-Myc might be responsible for stimulating mitochondrial function by modulating the consumption of alanine. The pyruvate consumption remained the same after the re-expression of c-Myc in HOMYC cells as compared to HO15. This finding is consistent with the analysis of mitochondrial respiration measured under both endogenous condition and in the presence of FCCP. c-Myc in HOMYC cells failed to reestablish an OCR similar to the one measured in TGR-1 cells. Furthermore, the maximal respiration measured with the uncoupler FCCP indicated an identical respiratory capacity in HO15 and HOMYC cells. The similar pyruvate uptake in HOMYC and HO15 cells might be explained by an identical PDH activity in both cell lines. Previous studies with NMR experiments by using ^{13}C-pyruvate demonstrated that endogenous c-Myc increases PDH activity in fibroblasts [32]. However, pyruvate carboxylase expression was increased in c-Myc $^{-/-}$ cells compared to the c-Myc $^{+/+}$ cells. Hence, difference in the pyruvate fluxes between those TGR-1 and HOMYC cells could be explained by the endogenous expression of c-Myc in TGR-1 cells and its exogenous expression in HOMYC which might not lead to the upregulation of PDH.

The second candidate that we considered for our combined analysis of secretomics and bioenergetics was KLF4. KLF4 is a transcription factor which was previously described as a tumor suppressor in lung and colon cancer [33–35], but also as an oncogene required for cell migration and invasion in breast cancer [36]. Little is known on the bioenergetics impact of this factor and we here found that KLF4 suppression triggers the Warburg effect. In contrast with c-Myc oncogenic inhibition in HO15 cells which reduced the respiratory capacity of the cells, KLF4 had no effect on oxygen consumption. Regarding secretomics, we identified an increase in AADA secretion which could be attributed to deregulation of fatty acid synthesis triggered by KLF4 inhibition. Our hypothesis is based on the observations that KO of KLF4 had no effect on mitochondrial respiration and ATP production. AADA is also considered as a glutamate analogue and promotes the proliferation of glial cells [37]. Given the negative correlation of KLF4 expression with cell proliferation, the important AADA secretion observed in KLF4 deficient cells might be because of lysine metabolism that contributes to the synthesis of acetyl-CoA probably for membrane synthesis necessary for cell growth. It will be relevant to study AADA fluxes on human cancer cells in order to consider the modulation of its production as a therapeutic strategy for cancer treatment. As compared to the oncogenes c-Myc and Oct1, KLF4 appears to play a role less important in cell metabolism. We observed an enhancement of glycolysis in the KLF4 deficient cells based on the increase of glucose uptake and lactate secretion. The enhancement of glycolytic phenotype observed in the KLF4$^{-/-}$ cells is consistent with the Warburg effect, which is a characteristic of proliferative cells. In addition, KLF4 expression has been reported to be decreased during the exponential phase of cell proliferation [38]. Furthermore, we provide evidence regarding KLF4 and its implication to the mitochondrial function with a similar RCR and identical ATP production capacity when comparing the wild type and the KLF4$^{-/-}$ cells. The metabolic signature observed in KLF4 deficient cells suggested an increase in protein synthesis probably necessary for proliferative cells. For example, the significant increase in hydroxyproline uptake observed might be required for collagen synthesis, criterion usually observed in fibroblasts localized in tumor microenvironment.

The third candidate was the Octamer transcription factor 1 (Oct1), a ubiquitous member of the POU-homeodomain family that functions

as a coregulator of the androgen receptor. Oct1 expression is increased in gastric carcinomas and lung adenocarcinomas [39,40]. We found that Oct1 deficiency leads to a reduced glycolytic phenotype with an inhibition of pyruvate uptake but increases the efficiency of the OXPHOS system. Therefore, the three analyzed oncogenes trigger specific bioenergetic changes that could explain in part the variability of the bioenergetics profile observed in tumors. We defined GABA as biomarker of Oct1 expression. The increase of GABA uptake, precursor of succinate, can explain the higher efficiency of mitochondrial respiration of Oct1 deficient cells as compare to the wild-type. The intracellular content of succinate among other TCA cycle intermediates has been reported to be decreased in Oct1 expressing cells [8]. Hence, the bioenergetics profile indicates that Oct1 expression reduces the uptake of GABA which leads to decrease in anaplerotic substrates content. The metabolic remodeling observed in Oct1 deficient cells was different from the other two oncogenes KLF4 and c-Myc. The inhibition of Oct1 expression in the MEFs was correlated with a decrease in glucose consumption and lactate secretion. Our results confirmed that the pyruvate uptake was also decreased in Oct1$^{-/-}$ cells compared to the wild-type MEFs. Oct1 is responsible for the regulation of pyruvate uptake and even oxidation, as well as most of the essential amino acids. The fact that Oct1 deficiency leads to an increase in RCR is in accordance with the higher mitochondrial capacity for ATP production as observed in our results. Shakaya et al. reported in their study that Oct1 deficiency induced metabolic changes which are consistent with a noncancer phenotypes because Oct1 inhibition by shRNA was responsible for a significant reduction in tumor forming potential of A549 cells in nude mice [8]. In summary, we can conclude that Oct1 expression is not only correlated with the Warburg effect, but also with a reduced OXPHOS efficiency.

In conclusion, we exemplified the importance of secretomics in the analysis of metabolic changes induced by oncogenes. c-Myc, Oct1 and KLF4 which play a role in the cell metabolism, regulate the energy state of the cells at different level. The MFP approach used in this study, permitted to highlight key metabolites such as isoleucine, AADA and GABA, for which the concentrations were correlated with both oncogene expression and cellular bioenergetic signatures. Our results suggest that this method when applied to tumors and their respective plasma could reveal biomarkers associated with energy metabolic changes in carcinogenesis. As a first step of cancer cells metabolic evaluation, we measured the uptake of glucose and pyruvate concomitantly with lactate secretion. Glucose consumption is widely used for tumor detection by PET scan (Positron Emission Tomography) which supports the importance of developing and refining secretomic analysis for cancer diagnosis. Hence, oncosecretomics could help in cancer diagnosis and provide information on the metabolic changes that occur inside the tumor. Since, no data was yet available on the potential interest of this methodology so we tested it first on the cell culture models that can be easily characterized from the bioenergetics standpoint. Secretomics performed on cells with variable expression of c-Myc, KLF4 and Oct1 allowed us to identify a set of new biomarkers: isoleucine, AADA and GABA. The uptake and secretion of those amino acids varied specifically with the modulation of oncogene expression and changed in correlation with the bioenergetics impact of those oncogenes. Our study illustrates the interest of secretomics for cancer biology and for the study of tumor bioenergetics.

Acknowledgements

We thank Dr. Dean Tantin (University of Utah School of Medicine), Dr John Sedivy (Brown University), Dr. Chi V. Dang (The Johns Hopkins University School of Medicine) and Dr. Vincent Yang (Emory University School of Medicine) for providing the cell lines in this study. This work was supported by funding from Rice University.

Appendix A. Supplementary data

Supplementary data to this article can be found online at http://dx.doi.org/10.1016/j.bbabio.2012.07.004.

References

[1] N. Bellance, P. Lestienne, R. Rossignol, Mitochondria: from bioenergetics to the metabolic regulation of carcinogenesis, Front. Biosci. 14 (2009) 4015–4034.
[2] C. Jose, N. Bellance, R. Rossignol, Choosing between glycolysis and oxidative phosphorylation: a tumor's dilemma? Biochim. Biophys. Acta 1807 (2011) 552–561.
[3] D. Nagrath, C. Caneba, T. Karedath, N. Bellance, Metabolomics for mitochondrial and cancer studies, Biochim. Biophys. Acta 1807 (2011) 650–663.
[4] T.J. Wang, M.G. Larson, R.S. Vasan, S. Cheng, E.P. Rhee, E. McCabe, G.D. Lewis, C.S. Fox, P.F. Jacques, C. Fernandez, C.J. O'Donnell, S.A. Carr, V.K. Mootha, J.C. Florez, A. Souza, O. Melander, C.B. Clish, R.E. Gerszten, Metabolite profiles and the risk of developing diabetes, Nat. Med. 17 (2011) 448–453.
[5] E.S. Ong, L. Zou, S. Li, P.Y. Cheah, K.W. Eu, C.N. Ong, Metabolic profiling in colorectal cancer reveals signaturemetabolic shifts during tumorigenesis,Mol. Cell. Proteomics (in press).
[6] A. Sreekumar, L.M. Poisson, T.M. Rajendiran, A.P. Khan, Q. Cao, J. Yu, B. Laxman, R. Mehra, R.J. Lonigro, Y. Li, M.K. Nyati, A. Ahsan, S. Kalyana-Sundaram, B. Han, X. Cao, J. Byun, G.S. Omenn, D. Ghosh, S. Pennathur, D.C. Alexander, A. Berger, J.R. Shuster, J.T. Wei, S. Varambally, C. Beecher, A.M. Chinnaiyan, Metabolomic profiles delineate potential role for sarcosine in prostate cancer progression, Nature 457 (2009) 910–914.
[7] M.K. Mateyak, A.J. Obaya, S. Adachi, J.M. Sedivy, Phenotypes of c-Myc-deficient rat fibroblasts isolated by targeted homologous recombination, Cell Growth Differ. 8 (1997) 1039–1048.
[8] A. Shakya, R. Cooksey, J.E. Cox, V. Wang, D.A. McClain, D. Tantin, Oct1 loss of function induces a coordinate metabolic shift that opposes tumorigenicity, Nat. Cell Biol. 11 (2009) 320–327.
[9] E.G. Hagos, A.M. Ghaleb, W.B. Dalton, A.B. Bialkowska, V.W. Yang, Mouse embryonic fibroblasts null for the Kruppel-like factor 4 gene are genetically unstable, Oncogene 28 (2009) 1197–1205.
[10] R.C. O'Hagan, M. Ohh, G. David, I.M. de Alboran, F.W. Alt, W.G. Kaelin Jr., R.A. DePinho, Myc-enhanced expression of Cul1 promotes ubiquitin-dependent proteolysis and cell cycle progression, Genes Dev. 14 (2000) 2185–2191.
[11] D. Kuystermans, M. Al-Rubeai, cMyc increases cell number through uncoupling of cell division from cell size in CHO cells, BMC Biotechnol. 9 (2009) 76.
[12] C.D. Folmes, T.J. Nelson, A. Martinez-Fernandez, D.K. Arrell, J.Z. Lindor, P.P. Dzeja, Y. Ikeda, C. Perez-Terzic, A. Terzic, Somatic oxidative bioenergetics transitions into pluripotency-dependent glycolysis to facilitate nuclear reprogramming, Cell Metab. 14 (2011) 264–271.
[13] D. Kuystermans, M.J. Dunn, M. Al-Rubeai, A proteomic study of cMyc improvement of CHO culture, BMC Biotechnol. 10 (2010) 25.
[14] N. Bellance, G. Benard, F. Furt, H. Begueret, K. Smolkova, E. Passerieux, J.P. Delage, J.M. Baste, P. Moreau, R. Rossignol, Bioenergetics of lung tumors: alteration of mitochondrial biogenesis and respiratory capacity, Int. J. Biochem. Cell Biol. 41 (2009) 2566–2577.
[15] D.R. Wise, R.J. DeBerardinis, A. Mancuso, N. Sayed, X.Y. Zhang, H.K. Pfeiffer, I. Nissim, E. Daikhin, M. Yudkoff, S.B. McMahon, C.B. Thompson, Myc regulates a transcriptional program that stimulates mitochondrial glutaminolysis and leads to glutamine addiction, Proc. Natl. Acad. Sci. U. S. A. 105 (2008) 18782–18787.
[16] W. Qian, B. Van Houten, Alterations in bioenergetics due to changes in mitochondrial DNA copy number, Methods 51 (2010) 452–457.
[17] O. Troyanskaya, M. Cantor, G. Sherlock, P. Brown, T. Hastie, R. Tibshirani, D. Botstein, R.B. Altman, Missing value estimation methods for DNA microarrays, Bioinformatics 17 (2001) 520–525.
[18] M. Barker, W. Rayens, Partial least squares for discrimination, J. Chemometr. 17 (2003) 166–173.
[19] K. Takahashi, S. Yamanaka, Induction of pluripotent stem cells from mouse embryonic and adult fibroblast cultures by defined factors, Cell 126 (2006) 663–676.
[20] S. Yamanaka, K. Takahashi, Induction of pluripotent stem cells from mouse fibroblast cultures, Tanpakushitsu Kakusan Koso 51 (2006) 2346–2351.
[21] H. Shim, C. Dolde, B.C. Lewis, C.S. Wu, G. Dang, R.A. Jungmann, R. Dalla-Favera, C.V. Dang, c-Myc transactivation of LDH-A: implications for tumor metabolism and growth, Proc. Natl. Acad. Sci. U. S. A. 94 (1997) 6658–6663.
[22] M. Yuneva, N. Zamboni, P. Oefner, R. Sachidanandam, Y. Lazebnik, Deficiency in glutamine but not glucose induces MYC-dependent apoptosis in human cells, J. Cell Biol. 178 (2007) 93–105.
[23] F. Li, Y. Wang, K.I. Zeller, J.J. Potter, D.R. Wonsey, K.A. O'Donnell, J.W. Kim, J.T. Yustein, L.A. Lee, C.V. Dang, Myc stimulates nuclearly encoded mitochondrial genes and mitochondrial biogenesis, Mol. Cell. Biol. 25 (2005) 6225–6234.
[24] O. Warburg, F. Wind, E. Negelein, The metabolism of tumors in the body, J. Gen. Physiol. 8 (1927) 519–530.
[25] O. Warburg, On the origin of cancer cells, Science 123 (1956) 309–314.
[26] C.V. Dang, A. Le, P. Gao, MYC-induced cancer cell energy metabolism and therapeutic opportunities, Clin. Cancer Res. 15 (2009) 6479–6483.
[27] M.L. Johansen, L.K. Bak, A. Schousboe, P. Iversen, M. Sorensen, S. Keiding, H. Vilstrup, A. Gjedde, P. Ott, H.S. Waagepetersen, The metabolic role of isoleucine

in detoxification of ammonia in cultured mouse neurons and astrocytes, Neurochem. Int. 50 (2007) 1042–1051.
[28] D. Nagrath, M. Avila-Elchiver, F. Berthiaume, A.W. Tilles, A. Messac, M.L. Yarmush, Soft constraints-based multiobjective framework for flux balance analysis, Metab. Eng. 12 (2010) 429–445.
[29] D. Nagrath, M. Avila-Elchiver, F. Berthiaume, A.W. Tilles, A. Messac, M.L. Yarmush, Integrated energy and flux balance based multiobjective framework for large-scale metabolic networks, Ann. Biomed. Eng. 35 (2007) 863–885.
[30] G. D'Antona, M. Ragni, A. Cardile, L. Tedesco, M. Dossena, F. Bruttini, F. Caliaro, G. Corsetti, R. Bottinelli, M.O. Carruba, A. Valerio, E. Nisoli, Branched-chain amino acid supplementation promotes survival and supports cardiac and skeletal muscle mitochondrial biogenesis in middle-aged mice, Cell Metab. 12 (2010) 362–372.
[31] S. El-Sayed, T. Bezabeh, O. Odlum, R. Patel, S. Ahing, K. MacDonald, R.L. Somorjai, I.C. Smith, An ex vivo study exploring the diagnostic potential of 1H magnetic resonance spectroscopy in squamous cell carcinoma of the head and neck region, Head Neck 24 (2002) 766–772.
[32] F. Morrish, N. Isern, M. Sadilek, M. Jeffrey, D.M. Hockenbery, c-Myc activates multiple metabolic networks to generate substrates for cell-cycle entry, Oncogene 28 (2009) 2485–2491.
[33] Y. Zhou, W.L. Hofstetter, Y. He, W. Hu, A. Pataer, L. Wang, J. Wang, L. Yu, B. Fang, S.G. Swisher, KLF4 inhibition of lung cancer cell invasion by suppression of SPARC expression, Cancer Biol. Ther. 9 (2010) 507–513.
[34] Z.Y. Chen, J.L. Shie, C.C. Tseng, Gut-enriched Kruppel-like factor represses ornithine decarboxylase gene expression and functions as checkpoint regulator in colonic cancer cells, J. Biol. Chem. 277 (2002) 46831–46839.
[35] D.T. Dang, X. Chen, J. Feng, M. Torbenson, L.H. Dang, V.W. Yang, Overexpression of Kruppel-like factor 4 in the human colon cancer cell line RKO leads to reduced tumorigenecity, Oncogene 22 (2003) 3424–3430.
[36] F. Yu, J. Li, H. Chen, J. Fu, S. Ray, S. Huang, H. Zheng, W. Ai, Kruppel-like factor 4 (KLF4) is required for maintenance of breast cancer stem cells and for cell migration and invasion, Oncogene 30 (2011) 2161–2172.
[37] M. Takeda, A. Takamiya, J.W. Jiao, K.S. Cho, S.G. Trevino, T. Matsuda, D.F. Chen, alpha-Aminoadipate induces progenitor cell properties of Muller glia in adult mice, Invest. Ophthalmol. Vis. Sci. 49 (2008) 1142–1150.
[38] X. Chen, D.C. Johns, D.E. Geiman, E. Marban, D.T. Dang, G. Hamlin, R. Sun, V.W. Yang, Kruppel-like factor 4 (gut-enriched Kruppel-like factor) inhibits cell proliferation by blocking G1/S progression of the cell cycle, J. Biol. Chem. 276 (2001) 30423–30428.
[39] R. Almeida, J. Almeida, M. Shoshkes, N. Mendes, P. Mesquita, E. Silva, I. Van Seuningen, C.A. Reis, F. Santos-Silva, L. David, OCT-1 is over-expressed in intestinal metaplasia and intestinal gastric carcinomas and binds to, but does not transactivate, CDX2 in gastric cells, J. Pathol. 207 (2005) 396–401.
[40] S. Reymann, J. Borlak, Transcription profiling of lung adenocarcinomas of c-myc-transgenic mice: identification of the c-myc regulatory gene network, BMC Syst. Biol. 2 (2008) 46.